




## Heat Transfer Enhancement Using $\text{Al}_2\text{O}_3$ , $\text{CuO}$ , and Hybrid $\text{Al}_2\text{O}_3$ – $\text{CuO}$ Nanofluids in Water and Ethylene Glycol–Water Mixtures in an Automotive Radiator

Chau Nguyen Minh 

Faculty of Vehicle and Energy Engineering, Thai Nguyen University of Technology, Thai Nguyen 24000, Viet Nam

Corresponding Author Email: [minhchau-ice@tnut.edu.vn](mailto:minhchau-ice@tnut.edu.vn)

Copyright: ©2025 The author. This article is published by IETA and is licensed under the CC BY 4.0 license (<http://creativecommons.org/licenses/by/4.0/>).

<https://doi.org/10.18280/ijht.430420>

### ABSTRACT

**Received:** 8 July 2025

**Revised:** 18 August 2025

**Accepted:** 25 August 2025

**Available online:** 31 August 2025

#### **Keywords:**

*nanofluid, radiator cooling, CFD, hybrid nanoparticles, heat transfer enhancement*

Effective thermal management in automotive radiators is crucial for engine performance, yet conventional coolants limit heat dissipation. This study presents a novel numerical investigation of the effects of three types of nanofluids ( $\text{Al}_2\text{O}_3$ /base fluid,  $\text{CuO}$ /base fluid and hybrid  $\text{Al}_2\text{O}_3$ – $\text{CuO}$ /base fluid; base fluids are pure water and a 40:60 ethylene glycol/water) on the heat transfer performance of automotive radiators. Numerical simulations were studied with Reynolds numbers from 250 to 1750 and nanoparticle concentrations from 1% to 7%. The results showed that the convective heat transfer coefficient was significantly improved when using nanofluids. The most significant enhancement was observed in the  $\text{Al}_2\text{O}_3$ –pure water nanofluid, with an improvement of up to 32% at  $\text{Re} = 1750$  and a nanoparticle concentration of 7%. The results also indicated that the relative improvement rate of the convective heat transfer coefficient for nanoparticles in the EG/W mixture was higher than in pure water. Furthermore, the findings suggested that to fully realise the potential of hybrid nanofluids, several factors, including nanoparticle mixing ratios, dispersion stability, interparticle interactions, and flow conditions, must be carefully optimised.

## 1. INTRODUCTION

Thanks to continuous advancements in science and engineering, internal combustion engines in modern automobiles have achieved high thermal efficiencies, driven by technologies such as turbocharging, direct fuel injection, and lean-burn combustion under optimized operating conditions. However, these engines are constantly subjected to high thermal loads; therefore, to maintain engine performance and longevity, effective thermal management becomes a key factor. To achieve this, the cooling system must dissipate excess heat, maintain the engine at its optimum operating temperature, and enable rapid thermal stabilization during start-up [1].

At the heart of the cooling system lies the radiator, which serves as the primary component responsible for rejecting heat generated during engine operation. A typical radiator comprises three main sections: (1) the upper tank, which receives hot coolant from the engine; (2) the lower tank, which supplies cooled fluid back to the engine; and (3) flat tubes with attached fins that facilitate heat exchange with ambient air. As coolant flows through the tubes, it is cooled by airflow passing over the fins. However, due to the flat geometry of the tubes and fins, the heat transfer area is limited, resulting in suboptimal thermal performance. Conventional coolants, typically a water and ethylene glycol (EG) mixture, offer benefits such as anti-freezing and elevated boiling points [2], but suffer from low thermal conductivity and poor performance under extreme or rapidly varying heat loads [3].

To solve this problem, several studies have focused on enhancing fin geometry (e.g., corrugated, perforated, or multi-layer fins) to increase the surface area for heat exchange [4–6]. While effective, these approaches are approaching their practical design limits [7, 8]. In light of rising fuel costs and the demand for increased energy efficiency, downsizing the cooling system, including the radiator, is a promising direction. However, reducing the radiator's size while relying on conventional coolant leads to a further drop in thermal performance due to inherent limitations in thermal conductivity.

Nanofluids, base fluids engineered with suspended nanoparticles, represent a promising solution for thermal management challenges. Their high surface-area-to-volume ratio and superior thermal properties enable significantly enhanced conductivity compared to conventional coolants [9–11]. In the automotive sector, nanofluids have shown potential for enhancing heat dissipation while facilitating system miniaturization. For instance, Leong et al. [12] reported that using a copper/EG nanofluid in automotive radiators increased the heat transfer rate and overall heat transfer coefficient by up to 3.8%. Peyghambarzadeh et al. [13] observed a 45% improvement in cooling efficiency using water/ $\text{Al}_2\text{O}_3$  nanofluids. Other studies involving  $\text{CuO}$ ,  $\text{Fe}_2\text{O}_3$  [14–16] or carbon nanotubes (CNTs) [17], have shown significant enhancements in the heat transfer coefficient (8–55%) and Nusselt number (up to 90.76%). Ferrão Teixeira Alves et al. [18] further demonstrated that  $\text{Al}_2\text{O}_3$ – $\text{CuO}$  hybrid nanofluids improved the Nusselt number by 16.64%. More complex

hybrid nanofluids, such as TiO<sub>2</sub>-Cu- Ag [19], ZnO-TiO<sub>2</sub> [20], Al<sub>2</sub>O<sub>3</sub>/CuO/water-EG [21], CuO-MgO-TiO<sub>2</sub> [22], have also shown promising results, with thermal performance improvements of up to 46%.

Building on these advancements, this study investigates the convective heat transfer performance of nanofluids containing Al<sub>2</sub>O<sub>3</sub>, CuO, and their 50:50 hybrid mixture, dispersed in two base fluids: pure water and a 60:40 water/ethylene glycol mixture. Nanoparticle volume concentrations of 1%, 3%, 5%, and 7% are examined. A representative tube model of a car radiator is simulated using ANSYS Fluent, employing CFD techniques to analyze heat transfer performance via the Nusselt number and convective heat transfer coefficient.

## 2. CALCULATION OF THERMOPHYSICAL PROPERTIES OF NANOFLUIDS

The thermophysical properties of nanofluids were estimated using well-established theoretical models that have been validated and widely applied in previous research [23, 24]. The investigated nanofluid systems include:

- Nanoparticles: Al<sub>2</sub>O<sub>3</sub>, CuO, and a hybrid mixture (50% Al<sub>2</sub>O<sub>3</sub> + 50% CuO);
- Base fluids: pure water and ethylene glycol/water mixtures with volume ratios of 20:80 and 40:60.

The thermophysical properties of the base fluids were obtained from established data sources [25, 26]. It is assumed that the nanoparticles are uniformly and stably dispersed within the base fluid, enabling the use of effective medium theory to estimate the bulk properties of the nanofluid. The following models were employed for the calculation:

Density:

$$\rho_{nf} = \phi \rho_p + (1 - \phi) \rho_{bf} \quad (1)$$

Specific heat capacity:

$$(\rho C_p)_{nf} = \phi (\rho C_p)_p + (1 - \phi) (\rho C_p)_{bf} \quad (2)$$

Thermal conductivity (Maxwell model for spherical particles):

$$k_{nf} = \frac{k_p + (\Phi - 1)k_{bf} - \phi(\Phi - 1)(k_{bf} - k_p)}{k_p + (\Phi - 1)k_{bf} + \phi(k_{bf} - k_p)} k_{bf} \quad (3)$$

where, the shape factor is assumed to be  $\Phi = 3$  for spherical particles [27, 28].

Viscosity (for pure water as the base fluid):

$$\mu_{nf} = \mu_{bf}(123\phi^2 + 7.3\phi + 1) \quad (4)$$

where, the indices “*nf*”, “*bf*”, and “*p*” denote nanofluid, base fluid, and particles, respectively.

In the case of ethylene glycol/water mixtures as the base fluid, the same equations remain valid for nanoparticle volume fractions up to 3%, as supported by Sharma et al. [29]. The Maxwell model was selected for its proven accuracy with spherical particles at low concentrations (up to 7%), as validated in prior studies [23, 24]. Factors such as Brownian motion and particle agglomeration were not incorporated, as the single-phase homogeneous approximation assumes stable dispersion and negligible dynamic effects under laminar flow conditions, consistent with the low nanoparticle fractions and validated models used here [30]. Future work could extend to

multiphase models for higher concentrations or unstable dispersions.

In addition to single-component nanofluids, this study also investigates hybrid nanofluids (Al<sub>2</sub>O<sub>3</sub>-CuO at a 50:50 ratio), which have demonstrated enhanced thermal performance. According to Sudarmadji et al. [31], such hybrid systems can achieve up to 83% improvement in heat transfer due to synergistic effects, including particle resonance and intensified Brownian motion.

The effective properties of hybrid nanofluids were computed using a weighted average approach:

Density of hybrid nanofluid:

$$\rho_{nf} = \phi_1 \rho_{p1} + \phi_2 \rho_{p2} + (1 - \phi_1 - \phi_2) \rho_{bf} \quad (5)$$

with  $\phi_1 = \phi_2 = \phi/2$ .

Specific heat capacity of hybrid nanofluid:

$$(\rho C_p)_{nf} = \phi_1 (\rho C_p)_{p1} + \phi_2 (\rho C_p)_{p2} + (1 - \phi_1 - \phi_2) (\rho C_p)_{bf} \quad (6)$$

where, *p1*, *p2* refer to Al<sub>2</sub>O<sub>3</sub> and CuO.

These models have been reported to agree well with experimental data in numerous studies [25, 32] and were adopted as input parameters for the CFD simulations conducted in ANSYS Fluent. The full list of thermophysical properties used in the simulations is summarized in Table 1.

**Table 1.** Thermal properties of base fluids, nanoparticles and nanofluids

Materials	Density- $\rho$ , (kg/m <sup>3</sup> )	Viscosity- $\mu$ , (kg/m.s)	Thermal conductivity-k, (W/m.K)	Specific heat-C <sub>p</sub> , (kJ/kgK)
Pure water	992	0.00065	0.633	4174
20:80% EG/W	1008	0.0019	0.58	4020
40:60% EG/W	1055.39	0.00226	0.412	3502
Al <sub>2</sub> O <sub>3</sub>	3960	-	40	773
CuO	6000	-	33	551

Note: EG/W - ethylene glycol/water

## 3. NUMERICAL SIMULATIONS

### 3.1 Geometry and mesh

The geometrical configuration of the automobile radiator is shown in Figure 1. The radiator consists of flat tubes integrated with corrugated fins to optimize heat transfer between the internal working fluid and ambient air. Each tube has principal dimensions of 21 mm (width, *a*), 4 mm (height, *b*), and 315 mm (length, *c*). The wall thickness is 0.2 mm. The thickness of the fin is 0.1 mm, and the number of fins on the tube is 34. As documented in prior research, these dimensions align with standard commercial automotive radiator designs [32].

### 3.2 Governing equation

The governing equations for fluid flow and heat transfer within the radiator are formulated and solved in Cartesian coordinates, as ANSYS Fluent adopts this coordinate system for implementing the conservation equations of mass,

momentum, and energy. The radiator geometry is fully defined and embedded into a structured computational mesh to ensure numerical accuracy and simulation results convergence [33].

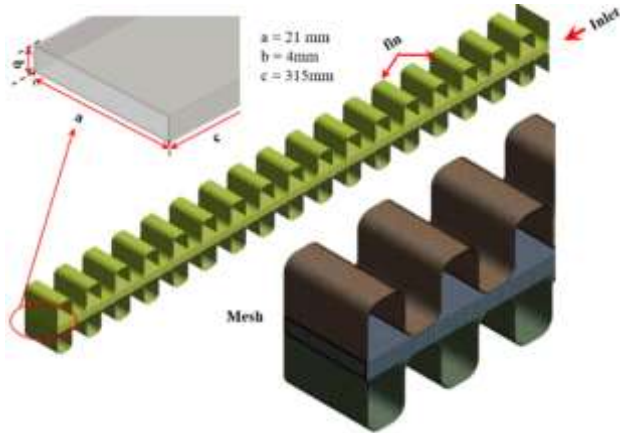


**Figure 1.** 3D geometry of the radiator tube (left) and computational mesh model (right)

Continuity equation:

The conservation of mass for incompressible flow is expressed as:

$$\frac{\partial}{\partial x_i}(\rho_{nf} V_i) = 0 \quad (7)$$

where,  $V_i$  is the component of the velocity vector in the  $i$ -th direction (m/s).

Momentum equation:

$$\frac{\partial}{\partial x_i}(\rho_{nf} V_j V_i) = -\frac{\partial p}{\partial x_j} + \frac{\partial p}{\partial x_j} \left( \mu_{nf} \left( \frac{\partial V_j}{\partial x_i} \right) \right) \quad (8)$$

where,  $\rho_{nf}$  is the density of the nanofluid (kg/m<sup>3</sup>),  $p$  is the pressure (Pa),  $\mu_{nf}$  is the dynamic viscosity of the nanofluid (kg/m.s) and  $i, j \in \{1, 2, 3\}$  represent the spatial coordinates.

Energy equation:

The conservation of energy for the nanofluid is given by:

$$\frac{\partial}{\partial x_i}(\rho_{nf} C_{pnf} V_i T) = \frac{\partial p}{\partial x_i} \left( K_{nf} \left( \frac{\partial T}{\partial x_i} \right) \right) \quad (9)$$

where,  $C_{pnf}$  is the specific heat capacity of the nanofluid (J/kg.K),  $T$  is the temperature of the fluid (K) và  $K_{nf}$  is the thermal conductivity of the nanofluid (W/m.K).

### 3.3 Boundary conditions

The numerical simulations investigated laminar flow conditions across Reynolds numbers (Re) of 250-1750 (specifically 250, 500, 750, 1000, 1250, 1500, and 1750). Comparative analysis of convective heat transfer coefficients ( $h$ ) between pure water and ethylene glycol/water (EG/W) base fluid was performed at four inlet velocities (0.05, 0.10, 0.15, and 0.20 m/s).

Boundary Conditions:

- Inlet: Uniform velocity profile with temperature fixed at 353.15 K (80°C)

- Outlet: Pressure outlet (0 Pa gauge pressure)
- Walls: No-slip condition for all solid boundaries
- Interfaces: Conservative interface flux at fluid-solid boundaries
- Ambient: Air temperature maintained at 303.15 K with external convective coefficient of 50 W/m<sup>2</sup>·K (representing vehicle speed of 72 km/h)

The hydraulic diameter of the flat tubes was calculated as 0.00613 m based on their cross-sectional dimensions (21 mm width × 4 mm height).

Modeling Assumptions:

- Incompressible nanofluid with constant density (pressure- and temperature-independent within the studied range);
- Laminar flow regime with negligible viscous dissipation effects;
- Single-phase homogeneous fluid approximation, validated by previous studies [30], for:
  - Well-dispersed nanoparticles
  - Effective thermophysical properties
  - Hydrothermal behavior comparable to pure liquids

Numerical scheme:

The finite volume method (FVM) in ANSYS Fluent 19.2 solved the governing equations (continuity, momentum, energy) with:

- Double-precision arithmetic
- SIMPLE algorithm for pressure-velocity coupling
- Second-order upwind discretization
- Convergence criterion: residuals < 10<sup>-6</sup> for all equations

### 3.4 Mesh independence study

To optimize the computational model, a mesh independence study was performed in ANSYS Fluent to (1) minimize computational cost while (2) ensuring solution accuracy. Multiple mesh configurations with progressively refined element densities were evaluated by monitoring the coolant outlet temperature as the convergence criterion (Figure 2). The second size (1,074,150 elements) is utilized in this study.

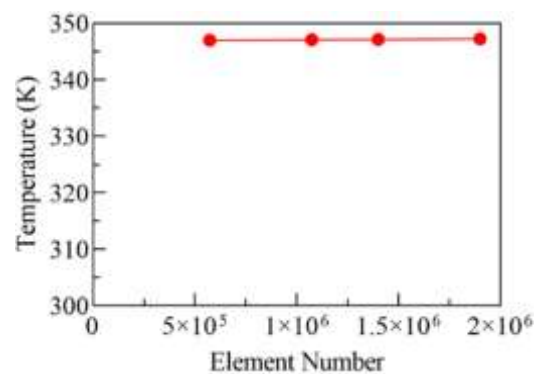


**Figure 2.** Mesh convergence analysis

## 4. RESULTS AND DISCUSSION

### 4.1 Calculation of average heat transfer coefficient and average Nusselt number

The average convective heat transfer coefficient  $h_{avg}$  and

average Nusselt number  $Nu_{avg}$  were determined using Newton's law of cooling and thermo-fluid parameters obtained from CFD simulations. The total heat transfer from the coolant to the inner tube wall is expressed as:

$$Q = h_{avg} A_s (T_b - T_s) \quad (10)$$

where,  $A_s$  is the inner surface area of the tube,  $T_s$  denotes the average tube wall temperature, and  $T_b$  is the average coolant temperature.

The average heat transfer coefficient was calculated directly from the heat flux density using:

$$h_{avg} = \frac{q''}{T_b - T_s} \quad (11)$$

Here,  $q''$  represents the mean heat flux density across the tube wall ( $W/m^2$ ), obtained from the Total Surface Heat Flux field using the Area-Weighted Average function (Surface Integrals tool) in Ansys Fluent. The tube wall temperature  $T_s$  was similarly determined by area-weighted averaging of the Wall Temperature field data. The mean fluid temperature  $T_b$  was computed as a mass-weighted average across the entire fluid domain using the Volume Integrals > Mass-Weighted Average function.

The average Nusselt number was subsequently calculated as:

$$Nu_{avg} = \frac{h_{avg} D_h}{k} \quad (12)$$

where,  $D_h$  is the hydraulic diameter and  $k$  is the thermal conductivity of the fluid.

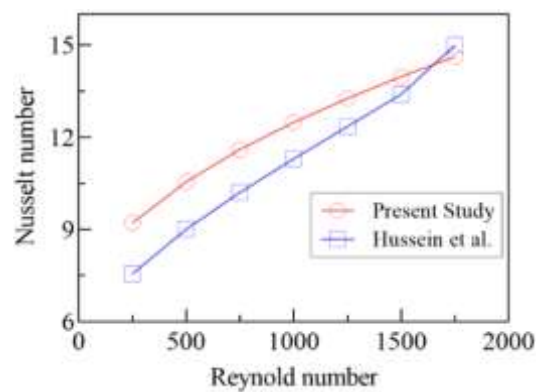
#### 4.2 Simulation model verification

To validate the accuracy of the CFD model, the present study replicated simulations using pure water as the working fluid, adopting the geometric configuration and boundary conditions reported by Hussein et al. [34]. The thermophysical properties of pure water were also taken from the same source. Unlike the original study, which simplified the model by neglecting the tube wall thickness and excluding the fins, the current model incorporates these features to more accurately represent the actual structure of an automotive radiator. Nusselt number data from the reference study were extracted using the WebPlotDigitizer software, as the original publication did not provide tabulated data. The simulation results were then compared with the reference data, as shown in Figure 3. The results demonstrate that the present model successfully reproduces the increasing trend of the Nusselt number with Reynolds number. The average deviation between the two datasets of Nusselt number is approximately 10.3%, which is considered acceptable in light of the differences in physical modeling and the potential uncertainties introduced during data extraction from graphs.

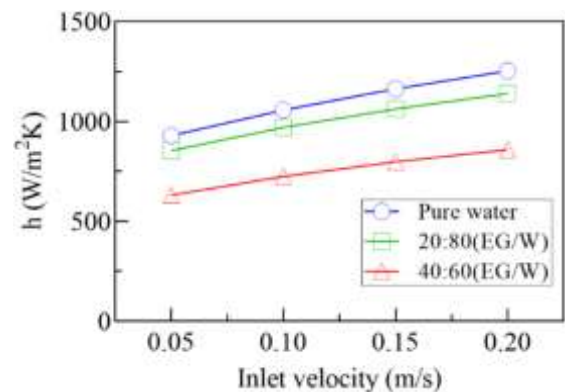
#### 4.3 Effect of ethylene glycol on the convective heat transfer coefficient

Figure 4 represents the variation of the convective heat transfer coefficient ( $h$ ) with inlet velocity for three working fluids: pure water, a 20:80 ethylene glycol/water (EG/W) mixture, and a 40:60 EG/W mixture. The results indicate that

$h$  decreases as the ethylene glycol content in the mixture increases. This observation agrees with the experimental work of Chen et al. [35], which demonstrated that ethylene glycol reduces heat transfer efficiency due to its lower thermal conductivity and higher viscosity. Pure water consistently exhibits the highest  $h$  value among the three fluids at any given inlet velocity. The 20:80 EG/W mixture shows intermediate performance, whereas the 40:60 EG/W mixture exhibits the lowest heat transfer coefficient across the investigated range of velocities. This behavior can be attributed to the combined effects of increasing viscosity and decreasing thermal conductivity as the ethylene glycol concentration rises, which hinder effective heat transfer between the liquid flow and the pipe wall. Moreover,  $h$  increases with inlet velocity in all cases, following the theory of forced convection heat transfer. Higher velocities enhance flow turbulence, thereby improving the convective heat transfer coefficient. However, the rate of increase in  $h$  is noticeably lower for mixtures with higher EG content, reflecting the detrimental effect of ethylene glycol on overall heat transfer performance.



**Figure 3.** Nusselt number versus Reynolds number for the current CFD model compared with Hussein et al. [34]



**Figure 4.** Effect of ethylene glycol concentration on the convective heat transfer coefficient

#### 4.4 Effect of $Al_2O_3$ and $CuO$ nanoparticle concentrations in pure water on the convective heat transfer coefficient

Figures 5 and 6 depict the variation of the convective heat transfer coefficient ( $h$ ) with Reynolds number for different concentrations of  $Al_2O_3$  and  $CuO$  nanoparticles dispersed in pure water. The investigated nanoparticle volume concentrations include  $\phi = 0$  (pure water), 0.01 (1%), 0.03 (3%), 0.05 (5%), and 0.07 (7%). The results indicate that the heat transfer coefficient increases markedly with rising



nanoparticle concentration across the entire range of Reynolds numbers considered. At a given Reynolds number, nanofluids containing  $\text{Al}_2\text{O}_3$  or  $\text{CuO}$  exhibit significantly higher  $h$  values compared to pure water. The enhancement effect becomes more pronounced at higher concentrations, particularly at  $\phi = 0.07$ , where the heat transfer coefficient reaches its maximum value within the investigated range. The maximum enhancements are approximately 32.18% for  $\text{Al}_2\text{O}_3$  and 28.51% for  $\text{CuO}$  relative to pure water (see Tables 2 and 3), demonstrating the significant impact of nanoparticle addition on the thermal performance of the base fluid.

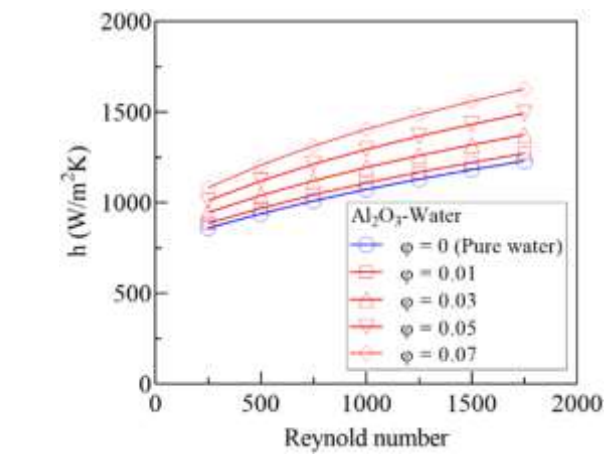
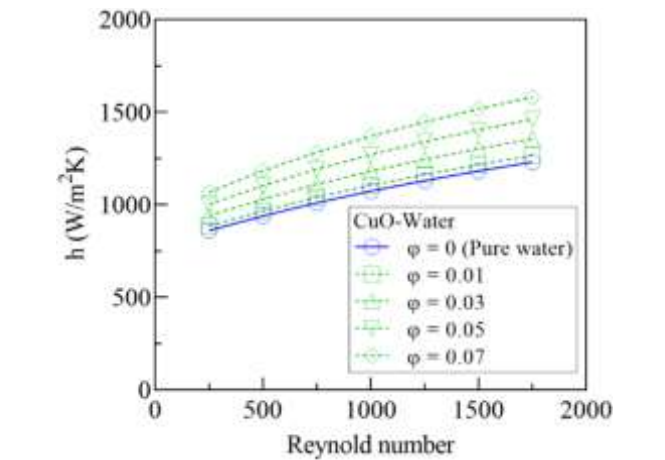


**Figure 5.** Effect of  $\text{Al}_2\text{O}_3$  nanoparticle concentration on  $h$  in pure water

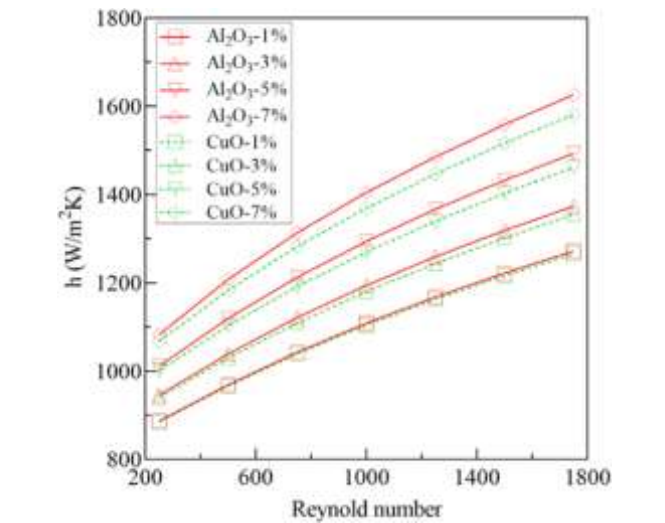
#### 4.5 Comparison of convective heat transfer coefficients of nanofluids containing $\text{Al}_2\text{O}_3$ and $\text{CuO}$ nanoparticles in pure water

Figure 7 illustrates the variation of the convective heat transfer coefficient with Reynolds number for nanofluid solutions comprising  $\text{Al}_2\text{O}_3$  and  $\text{CuO}$  nanoparticles at different volume concentrations (1%, 3%, 5%, and 7%) in pure water. Overall, both types of nanofluids exhibited a marked enhancement in heat transfer performance compared to pure water. This enhancement increased progressively with Reynolds number and nanoparticle concentration. A comparison between the two nanoparticle types revealed that the  $\text{Al}_2\text{O}_3$ -based nanofluid achieved higher heat transfer coefficients than the  $\text{CuO}$ -based nanofluid under identical

operating conditions. However, within the simulation parameters of this study, the maximum observed difference between the two nanofluids was approximately 3% (see Table 3), suggesting that the disparity in heat transfer performance remained relatively small within the investigated range.



**Figure 6.** Effect of  $\text{CuO}$  nanoparticle concentration on  $h$  in pure water



**Figure 7.** Comparison of convective heat transfer coefficients of nanofluids containing  $\text{Al}_2\text{O}_3$  and  $\text{CuO}$  nanoparticles in pure water

**Table 2.** Convective heat transfer coefficient ( $h$ ) of pure water at various Reynolds numbers

Re	250	500	750	1000	1250	1500	1750
$h$ ( $\text{W}/\text{m}^2\text{K}$ )	860.391	939.14	1010.04	1073.19	1130.11	1182.11	1230.26

**Table 3.** Heat transfer coefficients of pure water-based nanofluids at different concentrations

Re	$h$	Pure Water- $\text{Al}_2\text{O}_3$				Pure Water- $\text{CuO}$			
		1%	3%	5%	7%	1%	3%	5%	7%
250		886.89	945.73	1011.38	1083.10	885.13	940.16	1001.43	1068.00
500		969.39	1039.18	1119.47	1208.09	966.23	1029.81	1102.88	1183.56
750		1043.29	1121.68	1212.80	1313.64	1039.23	1109.61	1191.78	1282.97
1000		1108.10	1194.35	1294.11	1404.67	1104.23	1180.31	1269.83	1369.43
1250		1168.11	1259.44	1366.57	1485.39	1162.80	1243.81	1339.61	1446.39
1500		1222.13	1318.75	1432.44	1558.65	1216.29	1301.74	1403.12	1516.36
1750		1272.04	1373.57	1493.23	1626.19	1265.83	1355.33	1461.83	1580.95

**Table 4.** Heat transfer coefficients of 40:60 (EG/W)-based nanofluids at different concentrations

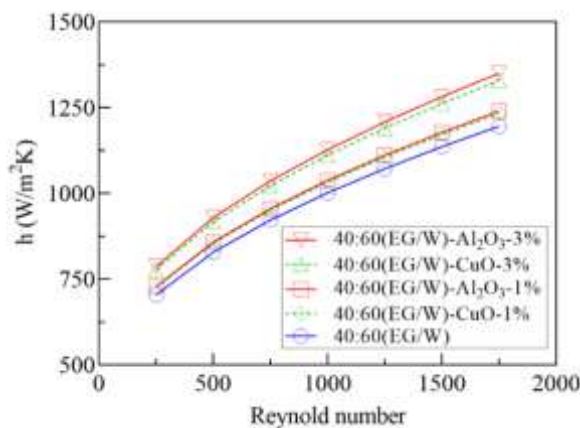
Re	h	40:60 (EG/W)	40:60 (EG/W)-Al <sub>2</sub> O <sub>3</sub>		40:60 (EG/W)-CuO	
			1%	3%	1%	3%
250		703.963	728.437	786.53	725.555	777.719
500		828.688	858.191	929.289	854.311	917.448
750		922.624	955.876	1036.693	951.263	1022.604
1000		1001.671	1038.111	1127.326	1032.859	1111.221
1250		1071.891	1111.206	1207.959	1105.329	1190.026
1500		1136.079	1178.006	1281.656	1171.602	1262.049
1750		1195.721	1240.055	1350.015	1233.168	1328.917

**Table 5.** Effect of Al<sub>2</sub>O<sub>3</sub> nanoparticles on heat transfer in water and EG/W solution at various Reynolds numbers

Re	h	Pure Water	40:60(EG/W)	Pure Water-Al <sub>2</sub> O <sub>3</sub>				40:60(EG/W)-Al <sub>2</sub> O <sub>3</sub>			
				1%	Enhancement (%)	3%	Enhancement (%)	1%	Enhancement (%)	3%	Enhancement (%)
250		860.39	703.96	886.89	3.08	945.73	9.92	728.44	3.48	786.53	11.73
500		939.14	828.69	969.39	3.22	1039.18	10.65	858.19	3.56	929.29	12.14
750		1010.04	922.62	1043.29	3.29	1121.68	11.05	955.88	3.6	1036.69	12.36
1000		1073.19	1001.67	1109	3.34	1194.35	11.29	1038.11	3.64	1127.33	12.54
1250		1130.11	1071.89	1168.11	3.36	1259.44	11.44	1111.21	3.67	1207.96	12.69
1500		1182.11	1136.08	1222.13	3.39	1318.75	11.56	1178.01	3.69	1281.66	12.81
1750		1230.26	1195.72	1272.04	3.4	1373.57	11.65	1240.06	3.71	1350.02	12.9

#### 4.6 Comparison of convective heat transfer coefficients of nanofluids containing Al<sub>2</sub>O<sub>3</sub> and CuO nanoparticles in a 40%EG/60%Water base fluid

Figure 8 illustrates the variation of the convective heat transfer coefficient ( $h$ ) with Reynolds number for nanofluids containing Al<sub>2</sub>O<sub>3</sub> and CuO nanoparticles at volume concentrations of 1% and 3%, using a base fluid of 40% ethylene glycol and 60% water (40%EG/60%Water). Similar to the results obtained with pure water, both nanofluids exhibited significant enhancements in the convective heat transfer coefficient compared to the base fluid without nanoparticles. This enhancement increased with Reynolds number and nanoparticle concentration.

**Figure 8.** Comparison of convective heat transfer coefficients of nanofluids containing Al<sub>2</sub>O<sub>3</sub> and CuO nanoparticles in a 40%EG/60%Water base fluid

However, consistent with previous observations, the CuO nanofluid demonstrated a lower improvement in heat transfer performance compared to the Al<sub>2</sub>O<sub>3</sub> nanofluid under identical conditions. Notably, when comparing the heat transfer enhancement efficiency of a nanofluid containing 3% Al<sub>2</sub>O<sub>3</sub> in two different base fluids at  $Re = 1750$ , it was found that the enhancement in the 40%EG/60%Water mixture was 12.9%,

which was higher than that in pure water (11.65%) (see Tables 4 and 5). This finding indicates that selecting a base fluid with an appropriate ethylene glycol ratio, combined with an optimal nanoparticle concentration, can yield superior heat transfer efficiency compared to using pure water as the dispersion medium.

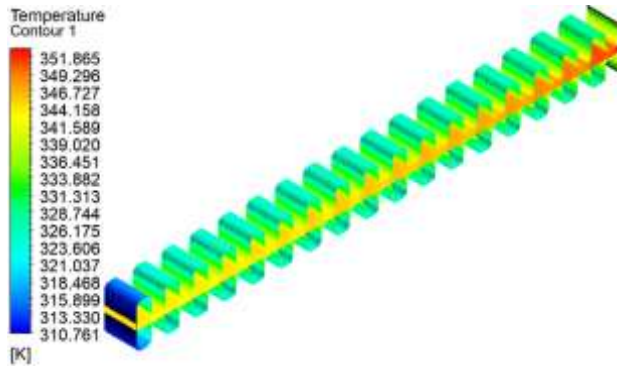
Table 5 presents the convective heat transfer performance of nanofluids containing Al<sub>2</sub>O<sub>3</sub> nanoparticles dispersed in two different base fluids: pure water and a 40:60 ethylene glycol/water (EG/W) mixture. The results were evaluated over a Reynolds number range of 250 to 1750, with nanoparticle volume concentrations of 1% and 3%. The addition of Al<sub>2</sub>O<sub>3</sub> nanoparticles significantly increased the convective heat transfer coefficient in both base fluids. At a concentration of 1%, the heat transfer efficiency improved from approximately 3.08% to 3.40% in pure water, and from 3.48% to 3.71% in the EG/W mixture. When the nanoparticle concentration increased to 3%, the efficiency gain became more pronounced, reaching 11.65% for pure water and 12.90% for EG/W at  $Re = 1750$ . These results highlight the positive and consistent effect of Al<sub>2</sub>O<sub>3</sub> nanoparticles in enhancing heat transfer performance across a range of flow rates.

Although pure water exhibited a higher absolute heat transfer coefficient due to its superior thermal conductivity, the relative improvement rate (%) resulting from the addition of nanoparticles was consistently higher in the EG/W mixture. This can be attributed to the inherently lower heat transfer capacity of EG/W, where the incorporation of nanoparticles produced a relatively more pronounced effect. For instance, at  $Re = 1500$  with a nanoparticle concentration of 3%, the enhancement reached 12.81% in EG/W compared to 11.56% in pure water.

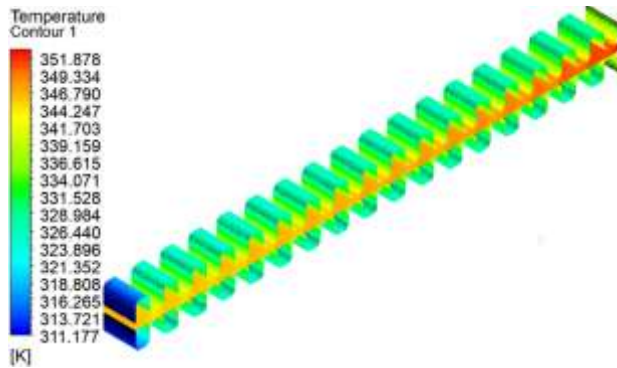
From an application standpoint, these findings suggest that Al<sub>2</sub>O<sub>3</sub> nanofluids in an EG/W medium can provide relatively greater benefits in terms of heat transfer efficiency, making them particularly suitable for systems that utilize base fluids with low inherent thermal conductivity. However, it is important to note that increasing the nanoparticle concentration may lead to higher viscosity and pressure losses, which could negatively impact the overall thermo-hydraulic

performance of the system. Therefore, future investigations should consider additional factors such as pressure drop and pumping power to obtain a more comprehensive assessment of operational efficiency.

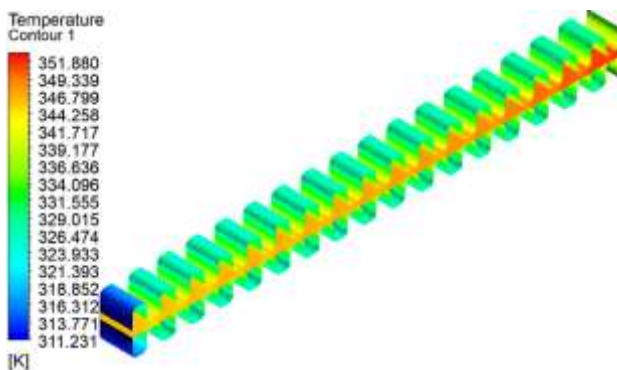
Moreover, in contrast to the findings reported by Sudarmadji et al. [31], where CuO nanofluids demonstrated superior heat transfer performance over Al<sub>2</sub>O<sub>3</sub>, the present study reveals that Al<sub>2</sub>O<sub>3</sub> outperforms CuO under steady flow conditions and at higher concentrations (3%). This disparity underscores that the heat transfer performance of different nanoparticle types is strongly influenced by specific operating conditions, channel geometry, and base fluid properties.



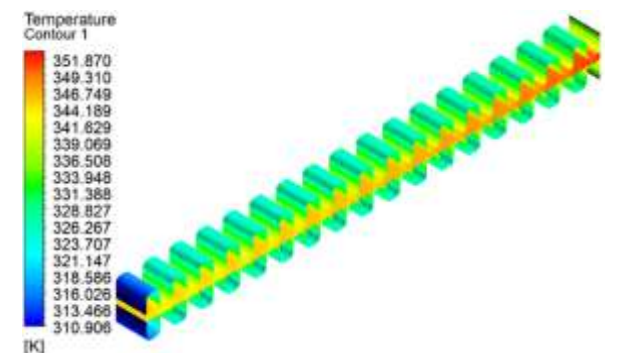
(a) Pure water



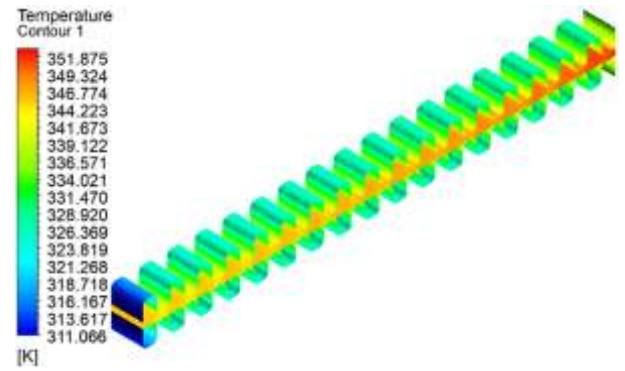
(b) Pure water-CuO-7%



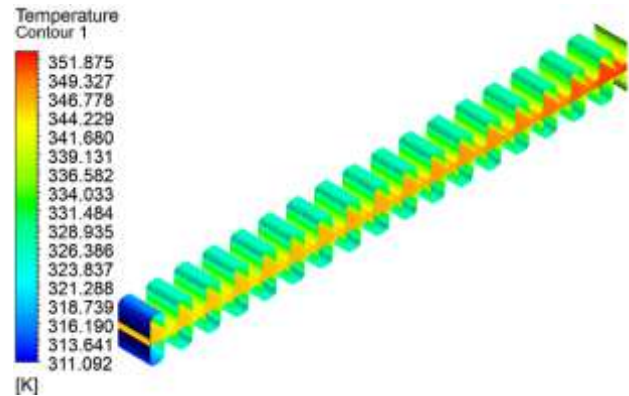
(c) Pure water- Al<sub>2</sub>O<sub>3</sub>-7%



(d) 40:60(EG/W)



(e) 40:60(EG/W)-CuO-3%



(f) 40:60(EG/W)-Al<sub>2</sub>O<sub>3</sub>-3%

**Figure 9.** Temperature distribution along the cooling tube for two types of nanofluids with different base fluids at  $Re = 1750$

Figure 9 illustrates the temperature distribution obtained from simulations of fluid flow in the cooling tube at a Reynolds number of  $Re = 1750$ . The analyzed cases involve nanofluids containing CuO and Al<sub>2</sub>O<sub>3</sub> nanoparticles at volume concentrations of 3% and 7%, dispersed in two base fluids: pure water and a 40:60 ethylene glycol/water mixture (EG/W).

The temperature contours depict the distribution of temperature along the tube length as the coolant circulates through the system. The results reveal a gradual decrease in temperature along the nanofluid flow direction, indicating heat transfer from the fluid to the tube wall and subsequently to the surrounding environment. These findings are consistent with the work of Tijani and bin Sudirman [32], where heat is transferred from the high-temperature coolant through the flat tube and fins via a combination of convective heat transfer within the fluid and conduction through the solid material. The continuous and uniform temperature profiles, without the presence of localized hot spots, suggest that the flow remains stable and that the heat transfer problem has been effectively resolved within the computational domain. Furthermore, the contour plots visually highlight the extent and intensity of heat exchange on the tube surface, thereby identifying the locations of effective cooling zones along the system's length.

#### 4.7 Comparison of heat transfer efficiency of three types of nanoparticles: CuO, Al<sub>2</sub>O<sub>3</sub>, and Al<sub>2</sub>O<sub>3</sub> + CuO in two base fluids

Figures 10 and 11 illustrate the variation of the convective heat transfer coefficient for three types of nanoparticles, CuO, Al<sub>2</sub>O<sub>3</sub>, and a hybrid mixture of Al<sub>2</sub>O<sub>3</sub> + CuO, dispersed in two base fluids: pure water and a 40:60 ethylene glycol/water



(EG/W) solution. In all cases, the nanoparticle concentration was maintained at 3% by volume, while the Reynolds number ranged from 250 to 1750 to simulate different flow regimes.

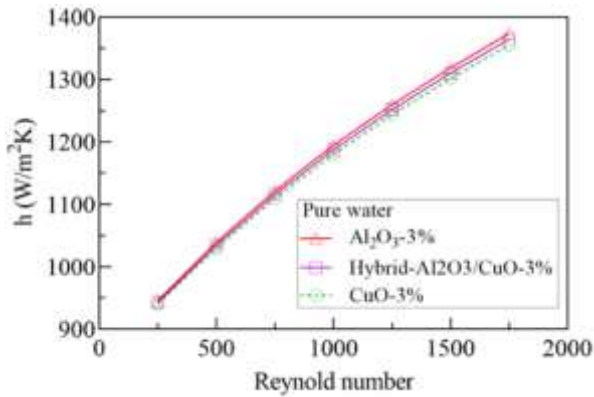


**Figure 10.** Comparison of heat transfer efficiency of three types of nanoparticles in pure water

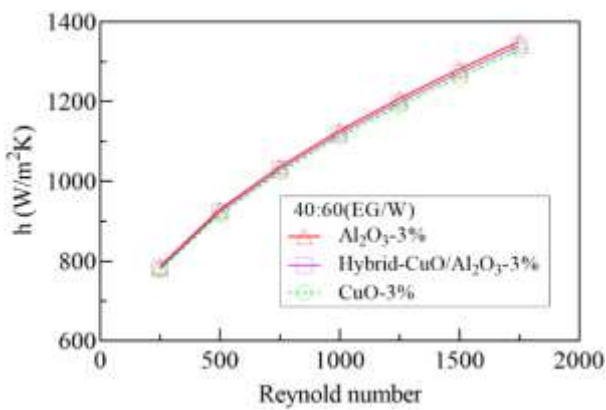


**Figure 11.** Comparison of heat transfer efficiency of three types of nanoparticles in the base fluid (40:60 EG/W)

The simulation results reveal a consistent trend across both base fluids: The Al<sub>2</sub>O<sub>3</sub> nanofluid exhibits the highest heat transfer coefficient, followed by the hybrid nanofluid (Al<sub>2</sub>O<sub>3</sub> + CuO), with the CuO nanofluid showing the lowest performance. This trend remains largely unaffected by changes in Reynolds number, suggesting that the type of nanoparticle has a more pronounced influence on heat transfer enhancement than the flow rate.

Although hybrid nanofluids are often expected to combine the advantages of their individual components, the present findings indicate that the heat transfer performance of the Al<sub>2</sub>O<sub>3</sub> + CuO hybrid is not superior to that of the pure Al<sub>2</sub>O<sub>3</sub> nanofluid. The lower performance of the Al<sub>2</sub>O<sub>3</sub>-CuO hybrid nanofluid compared to pure Al<sub>2</sub>O<sub>3</sub> may be attributed to the fixed 50:50 mixing ratio used in this study. This mixing ratio may not be optimal for maximizing synergistic thermal effects. Additionally, particle-particle interactions and possible reduction in effective thermal conductivity due to CuO's lower thermal conductivity than Al<sub>2</sub>O<sub>3</sub> could also contribute. Prior studies [18, 21] indicate that hybrid nanofluids only outperform single-component nanofluids when composition, dispersion stability, and flow conditions are carefully optimized. This suggests that the enhancement mechanism in nanofluids is not simply additive; rather, it depends on several factors, including the mixing ratio of the constituent

nanoparticles, their dispersion stability in the base fluid, particle-particle interactions, and specific flow conditions. Some previous studies have also reported that hybrid nanofluids demonstrate significant performance improvements only when configuration parameters and operating conditions are carefully optimized. Therefore, the design and application of hybrid nanofluids should be approached comprehensively and selectively, rather than assuming inherently superior performance.

## 5. CONCLUSIONS

A numerical study was conducted to determine the effect of three types of nanofluids (Al<sub>2</sub>O<sub>3</sub>/base fluid, CuO/base fluid, and hybrid Al<sub>2</sub>O<sub>3</sub> – CuO/base fluid; base fluids are pure water and a 40:60 ethylene glycol/water mixture) on the heat transfer coefficient enhancement of a flat tube integrated with corrugated fins. This study provides the first comprehensive comparative analysis of Al<sub>2</sub>O<sub>3</sub>, CuO, and hybrid Al<sub>2</sub>O<sub>3</sub>-CuO nanofluids in pure water and EG/W mixtures. The results show that Al<sub>2</sub>O<sub>3</sub> nanofluids achieve up to a 32% improvement in performance, surpassing even the hybrid nanofluids under the tested conditions. These findings advance nanofluid applications in automotive cooling by demonstrating the importance of base fluid selection for relative efficiency gains. Based on the results, the main conclusions of this study can be summarised as follows:

- Nanofluids significantly improve the convective heat transfer coefficient of automotive radiators. The increase in convective heat transfer coefficient is linearly proportional to both the nanoparticle concentration and the Reynolds number. Among the three nanofluids, the Al<sub>2</sub>O<sub>3</sub>-pure water nanofluid exhibited the highest enhancement, with an increase of up to 32% at Re = 1750 and a nanoparticle concentration of 7%.

- The hybrid nanofluid did not demonstrate a clear advantage over the mono Al<sub>2</sub>O<sub>3</sub> nanofluid. This suggests that heat transfer enhancement depends not only on particle composition but also on the mixing ratio, dispersion properties, and flow conditions.

- Although nanofluids based on pure water exhibited higher absolute heat transfer coefficients, those based on EG/W showed a relatively greater percentage improvement (e.g., 12.9% vs. 11.7% for Al<sub>2</sub>O<sub>3</sub> at Re = 1750), highlighting their potential for applications involving low thermal conductivity base fluids.

- The temperature on the tube wall gradually decreased along the flow direction of the nanofluid, confirming that both convective and conductive heat transfer processes were effective. Furthermore, no abnormal temperature locations were observed on the tube wall. This confirmed that the flow was stable and that the numerical model was well constructed.

While this numerical study demonstrates significant heat transfer enhancements, limitations of this work include the assumption of ideal nanofluid stability, neglecting long-term issues such as particle sedimentation or agglomeration in real-world applications. Additionally, the study did not account for the cost implications of nanoparticle synthesis and integration into automotive systems, which could affect practical feasibility. Future research should address these through experimental stability tests, economic analyses, and pressure drop and pumping power assessments for comprehensive thermo-hydraulic optimization.



## ACKNOWLEDGMENT

The authors gratefully acknowledge the support of Thai Nguyen University of Technology through Project T2024-TS22.

## REFERENCES

- [1] Kaleli, A. (2020). Development of the predictive based control of an autonomous engine cooling system for variable engine operating conditions in SI engines: design, modeling and real-time application. *Control Engineering Practice*, 100: 104424. <https://doi.org/10.1016/j.conengprac.2020.104424>
- [2] Oliet, C., Oliva, A., Castro, J., Pérez-Segarra, C.D. (2007). Parametric studies on automotive radiators. *Applied Thermal Engineering*, 27(11-12): 2033-2043. <https://doi.org/10.1016/j.applthermaleng.2006.12.006>
- [3] Kulkarni, D.P., Vajjha, R.S., Das, D.K., Oliva, D. (2008). Application of aluminum oxide nanofluids in diesel electric generator as jacket water coolant. *Applied Thermal Engineering*, 28(14): 1774-1781. <https://doi.org/10.1016/j.applthermaleng.2007.11.017>
- [4] Chang, Y.J., Hsu, K.C., Lin, Y.T., Wang, C.C. (2243). A generalized friction correlation for louver fin geometry. *International Journal of Heat and Mass Transfer*, 43(12): 2237-2243. [https://doi.org/10.1016/S0017-9310\(99\)00289-6](https://doi.org/10.1016/S0017-9310(99)00289-6)
- [5] Wang, C.C. (1999). Investigation of wavy fin-and-tube heat exchangers: A contribution to databank. *Experimental Heat Transfer*, 12(1): 73-89. <https://doi.org/10.1080/089161599269825>
- [6] Wieting, A.R. (1975). Empirical correlations for heat transfer and flow friction characteristics of rectangular offset-fin plate-fin heat exchangers. *Journal of Heat Transfer*, 97(3): 488-490. <https://doi.org/10.1115/1.3450412>
- [7] Mukkamala, Y. (2017). Contemporary trends in thermo-hydraulic testing and modeling of automotive radiators deploying nano-coolants and aerodynamically efficient air-side fins. *Renewable and Sustainable Energy Reviews*, 76: 1208-1229. <https://doi.org/10.1016/j.rser.2017.03.106>
- [8] Alam, T., Kim, M.H. (2018). A comprehensive review on single phase heat transfer enhancement techniques in heat exchanger applications. *Renewable and Sustainable Energy Reviews*, 81: 813-839. <https://doi.org/10.1016/j.rser.2017.08.060>
- [9] Yu, W.H., France, D.M., Routbort, J.L., Choi, S.U.S. (2008). Review and comparison of nanofluid thermal conductivity and heat transfer enhancements. *Heat Transfer Engineering*, 29(5): 432-460. <https://doi.org/10.1080/01457630701850851>
- [10] Bacha, H.B., Ullah, N., Hamid, A., Shah, N.A. (2024). A comprehensive review on nanofluids: Synthesis, cutting-edge applications, and future prospects. *International Journal of Thermofluids*, 22: 100595. <https://doi.org/10.1016/j.ijft.2024.100595>
- [11] Altammar, K.A. (2023). A review on nanoparticles: characteristics, synthesis, applications, and challenges. *Frontiers in Microbiology*, 14: 1-20. <https://doi.org/10.3389/fmicb.2023.1155622>
- [12] Leong, K.Y., Saidur, R., Kazi, S.N., Mamun, A.H. (2010). Performance investigation of an automotive car radiator operated with nanofluid-based coolants (nanofluid as a coolant in a radiator). *Applied Thermal Engineering*, 30(17-18): 2685-2692. <https://doi.org/10.1016/j.applthermaleng.2010.07.019>
- [13] Peyghambarzadeh, S.M., Hashemabadi, S.H., Jamnani, M.S., Hoseini, S.M. (2011). Improving the cooling performance of automobile radiator with Al<sub>2</sub>O<sub>3</sub>/water nanofluid. *Applied Thermal Engineering*, 31(10): 1833-1838. <https://doi.org/10.1016/j.applthermaleng.2011.02.029>
- [14] Peyghambarzadeh, S.M., Hashemabadi, S.H., Naraki, M., Vermahmoudi, Y. (2013). Experimental study of overall heat transfer coefficient in the application of dilute nanofluids in the car radiator. *Applied Thermal Engineering*, 52(1): 8-16. <https://doi.org/10.1016/j.applthermaleng.2012.11.013>
- [15] Naraki, M., Peyghambarzadeh, S.M., Hashemabadi, S.H., Vermahmoudi, Y. (2013). Parametric study of overall heat transfer coefficient of CuO/water nanofluids in a car radiator. *International Journal of Thermal Sciences*, 66: 82-90. <https://doi.org/10.1016/j.ijthermalsci.2012.11.013>
- [16] Heris, S.Z., Shokrgozar, M., Poorpharhang, S., Shanbedi, M., Noie, S.H. (2014). Experimental study of heat transfer of a car radiator with CuO/ethylene glycol-water as a coolant. *Journal of Dispersion Science and Technology*, 35(5): 677-684. <https://doi.org/10.1080/01932691.2013.805301>
- [17] Chougule, S.S., Sahu, S.K. (2014). Comparative study of cooling performance of automobile radiator using Al<sub>2</sub>O<sub>3</sub>-water and carbon nanotube-water nanofluid. *Journal of Nanotechnology in Engineering and Medicine*, 5(1): 010901. <https://doi.org/10.1115/1.4026971>
- [18] Ferrão Teixeira Alves, L.O., Henríquez, J.R., da Costa, J.Á.P., Abramchuk, V. (2022). Comparative performance analysis of internal combustion engine water jacket coolant using a mix of Al<sub>2</sub>O<sub>3</sub> and CuO-based nanofluid and ethylene glycol. *Energy*, 250: 123832. <https://doi.org/10.1016/j.energy.2022.123832>
- [19] Soylu, S.K., Atmaca, İ., Asiltürk, M., Doğan, A. (2019). Improving heat transfer performance of an automobile radiator using Cu and Ag doped TiO<sub>2</sub> based nanofluids. *Applied Thermal Engineering*, 157: 113743. <https://doi.org/10.1016/j.applthermaleng.2019.113743>
- [20] Elibol, E.A., Gonulacar, Y.E., Aktas, F., Tigli, B. (2024). Effect of using a ZnO-TiO<sub>2</sub>/water hybrid nanofluid on heat transfer performance and pressure drop in a flat tube with louvered finned heat exchanger. *Journal of Thermal Analysis and Calorimetry*, 149(15): 8665-8680. <https://doi.org/10.1007/s10973-024-13346-7>
- [21] Tahat, M.S., Benim, A.C. (2017). Experimental analysis on thermophysical properties of Al<sub>2</sub>O<sub>3</sub>/CuO hybrid nano fluid with its effects on flat plate solar collector. *Defect and Diffusion Forum*, 374: 148-156. <https://doi.org/10.4028/www.scientific.net/DDF.374.148>
- [22] Kumar, A., Hassan, M.A. (2024). Heat transfer in flat tube car radiator with CuO-MgO-TiO<sub>2</sub> ternary hybrid nanofluid. *Powder Technology*, 434: 119275. <https://doi.org/10.1016/j.powtec.2023.119275>
- [23] Duangthongsuk, W., Wongwises, S. (2008). Effect of thermophysical properties models on the predicting of the convective heat transfer coefficient for low

- concentration nanofluid. *International Communications in Heat and Mass Transfer*, 35(10): 1320-1326. <https://doi.org/10.1016/j.icheatmasstransfer.2008.07.015>
- [24] Kole, M., Dey, T.K. (2010). Viscosity of alumina nanoparticles dispersed in car engine coolant. *Experimental Thermal and Fluid Science*, 34(6): 677-683. <https://doi.org/10.1016/j.expthermflusci.2009.12.009>
- [25] Peyghambarzadeh, S.M., Hashemabadi, S.H., Hoseini, S.M., Jamnani, M.S. (2011). Experimental study of heat transfer enhancement using water/ethylene glycol based nanofluids as a new coolant for car radiators. *International Communications in Heat and Mass Transfer*, 38(9): 1283-1290. <https://doi.org/10.1016/j.icheatmasstransfer.2011.07.002>
- [26] Devireddy, S., Mekala, C.S.R., Veeredhi, V.R. (2016). Improving the cooling performance of automobile radiator with ethylene glycol water based TiO<sub>2</sub> nanofluids. *International Communications in Heat and Mass Transfer*, 78: 121-126. <https://doi.org/10.1016/j.icheatmasstransfer.2016.09.002>
- [27] Qi, W.H., Wang, M.P., Liu, Q.H. (2005). Shape factor of nonspherical nanoparticles. *Journal of Materials Science*, 40(9-10): 2737-2739. <https://doi.org/10.1007/s10853-005-2119-0>
- [28] Wang, J., Yang, X., Klemeš, J.J., Tian, K., Ma, T., Sunden, B. (2023). A review on nanofluid stability: preparation and application. *Renewable and Sustainable Energy Reviews*, 188: 113854. <https://doi.org/10.1016/j.rser.2023.113854>
- [29] Sharma, K.V., Suleiman, A., Hassan, H.S.B., Hegde, G. (2017). Considerations on the Thermophysical Properties of Nanofluids. In: Korada, V., Hisham B Hamid, N. (eds) *Engineering Applications of Nanotechnology. Topics in Mining, Metallurgy and Materials Engineering*. Springer, Cham. [https://doi.org/10.1007/978-3-319-29761-3\\_2](https://doi.org/10.1007/978-3-319-29761-3_2)
- [30] Maïga, S.E.B., Palm, S.J., Nguyen, C.T., Roy, G., Galanis, N. (2005). Heat transfer enhancement by using nanofluids in forced convection flows. *International Journal of Heat and Fluid Flow*, 26(4): 530-546. <https://doi.org/10.1016/j.ijheatfluidflow.2005.02.004>
- [31] Sudarmadji, S., Irawan, B., Susilo, S.H. (2022). The effect of hybrid nanofluid CuO-TiO<sub>2</sub> on radiator performance. *Eastern-European Journal of Enterprise Technologies*, 4(5): 21-29. <https://doi.org/10.15587/1729-4061.2022.263649>
- [32] Tijani, A.S., bin Sudirman, A.S. (2018). Thermophysical properties and heat transfer characteristics of water/anti-freezing and Al<sub>2</sub>O<sub>3</sub>/CuO based nanofluid as a coolant for car radiator. *International Journal of Heat and Mass Transfer*, 118: 48-57. <https://doi.org/10.1016/j.ijheatmasstransfer.2017.10.083>
- [33] Huminic, G., Huminic, A. (2013). Numerical analysis of laminar flow heat transfer of nanofluids in a flattened tube. *International Communications in Heat and Mass Transfer*, 44: 52-57. <https://doi.org/10.1016/j.icheatmasstransfer.2013.03.003>
- [34] Hussein, A.M., Bakar, R.A., Kadirgama, K. (2014). Study of forced convection nanofluid heat transfer in the automotive cooling system. *Case Studies in Thermal Engineering*, 2: 50-61. <https://doi.org/10.1016/j.csite.2013.12.001>
- [35] Chen, H.Y., Suzuki, T., Asano, K., Shindo, R., Homma, A., Kimata, N., Nakaya, T., Nakamura, K., Yilmaz, E., Ichianagi, M. (2021). Effects of water and 50% ethylene-glycol coolant characteristics on nucleate boiling heat transfer in IC engine cooling system. *International Journal of Automotive Engineering*, 12(3): 78-85. [https://doi.org/10.20485/jsaeijae.12.3\\_78](https://doi.org/10.20485/jsaeijae.12.3_78)

## NOMENCLATURE

A	surface area (m <sup>2</sup> )
C <sub>p</sub>	specific heat capacity, J. kg <sup>-1</sup> . K <sup>-1</sup>
D <sub>h</sub>	hydraulic diameter, m
h	convective heat transfer coefficient, W.m <sup>-2</sup> .K <sup>-1</sup>
k	thermal conductivity, W.m <sup>-1</sup> . K <sup>-1</sup>
Nu	Nusselt number
p	pressure, Pa
Q	heat transfer rate, W
q"	heat flux, W.m <sup>-2</sup>
Re	Reynolds number
T	temperature, K
V	velocity, m.s <sup>-1</sup>

## Greek symbols

φ	nanoparticle volume fraction (%)
μ	dynamic viscosity kg.m <sup>-1</sup> .s <sup>-1</sup>
ρ	density, kg.m <sup>-3</sup>

## Subscripts

avg	average value
bf	base fluid
nf	nanofluid
p	nanoparticle
s	surface

## Abbreviations

CFD	computational fluid dynamics
EG/W	ethylene glycol/water mixture
FVM	finite volume method
SIMPLE	Semi-Implicit Method for Pressure-Linked Equations (algorithm)